Regulation of Secondary Cell Wall Development by Cortical Microtubules during Tracheary Element Differentiation in Arabidopsis Cell Suspensions[1][w]

Yoshihisa Oda, Tetsuro Mimura, and Seiichiro Hasezawa*

Department of Integrated Biosciences, Graduate School of Frontier Sciences, The University of Tokyo, Kashiwa, Chiba 277–8562, Japan (Y.O., S.H.); and Department of Biology, Faculty of Sciences, Kobe University, Nada-ku, Kobe 657–8501, Japan (T.M.)

Cortical microtubules participate in the deposition of patterned secondary walls in tracheary element differentiation. In this study, we established a system to induce the differentiation of tracheary elements using a transgenic Arabidopsis (*Arabidopsis thaliana*) cell suspension stably expressing a green fluorescent protein-tubulin fusion protein. Approximately 30% of the cells differentiated into tracheary elements 96 h after culture in auxin-free media containing 1 μM brassinolide. With this differentiation system, we have been able to time-sequentially elucidate microtubule arrangement during secondary wall thickening. The development of secondary walls could be followed in living cells by staining with fluorescein-conjugated wheat germ agglutinin, and the three-dimensional structures of the secondary walls could be simultaneously analyzed. A single microtubule bundle first appeared beneath the narrow secondary wall and then developed into two separate bundles locating along both sides of the developing secondary wall. Microtubule inhibitors affected secondary wall thickening, suggesting that the pair of microtubule bundles adjacent to the secondary wall played a crucial role in the regulation of secondary wall development.

Tracheary elements, known as components of xylem vessels, are equipped with elaborately patterned secondary cell walls under the primary cell walls, which give rise to their characteristic appearances. In contrast with primary cell walls, secondary walls are comparatively thick and stout due to their high cellulose content and their lignin and hemicellulose deposits, and provide the tracheary elements with enough strength to withstand high negative pressure within the vessels (Ye, 2002).

Cortical microtubules are known to participate in the regulation of secondary wall deposition. The microtubules lying directly beneath the secondary walls have been observed for over four decades by transmission electron microscopy in several plant species (Hepler and Newcomb, 1964; Wooding and Northcote, 1964; Pickett-Heaps, 1966; Pickett-Heaps and Northcote, 1966; Hardham and Gunning, 1979). The clustering of these microtubules is found to precede cell wall thickening and to be orientated parallel with the cellulose microfibrils and patterned secondary walls. If microtubules were destroyed by treatment with particular agents, irregular secondary walls could be observed (Pickett-Heaps, 1967; Hepler and Fosket, 1971; Brower and Hepler, 1976; Hardham and Gunning, 1980; Hepler, 1981).

The differentiation of tracheary elements can be induced semisynchronously in zinnia (*Zinnia elegans*) mesophyll cells (Fukuda and Komamine, 1980a). Zinnia mesophyll cells are useful materials not only for biochemical and molecular studies but also for cytological analyses because the tracheary elements are formed from single cells (Fukuda, 1992, 1997). Indirect immunofluorescent staining has revealed that microtubule orientations change dramatically from longitudinal to lateral orientations during the differentiation of cultured zinnia cells (Fukuda and Kobayashi, 1989). Treatment with the microtubule depolymerization inhibitor taxol is found to block this change and to consequently result in the formation of longitudinal secondary walls, reflecting the microtubule orientation at the time of inhibitor addition (Falconer and Seagull, 1985a, 1985b). Hence, the microtubules appear to decide the pattern of secondary wall deposition.

Previous studies of microtubules and secondary walls have been restricted to observations in chemically fixed cells. Therefore, the sequence of microtubule structures during secondary wall thickening could not be investigated in detail. Recently, observation of microtubules by the expression of green fluorescent protein (GFP)-tubulin fusion proteins, especially in stable transformants, has enabled time-lapse observations of microtubules in living cells and revealed several novel structures, dynamics, and functions of microtubules (Yoneda et al., 2003). For

[1] This work was supported in part by a Grant-in-Aid for Scientific Research on Priority Areas from The Ministry of Education, Culture, Sports, Science and Technology, Japan (grant no. 15031209 to S.H.).

* Corresponding author; e-mail hasezawa@k.u-tokyo.ac.jp; fax 81–4–7136–3706.

[w] The online version of this article contains Web-only data.

Article, publication date, and citation information can be found at www.plantphysiol.org/cgi/doi/10.1104/pp.104.052613.

instance, the processes of the transition of cortical microtubule orientations (Ueda and Matsuyama, 2000) and the treadmilling of cortical microtubules (Shaw et al., 2003) have been described in transgenic Arabidopsis (*Arabidopsis thaliana*). Microtubule dynamics throughout cell division have also been observed in transgenic Arabidopsis cell suspensions and transgenic tobacco (*Nicotiana tabacum*) cv Bright Yellow-2 (BY-2) cells. The processes of the development of phragmoplast microtubules (Ueda et al., 2003) and the reorganization of cortical microtubules at the M/G_1 phase (Hasezawa et al., 2000; Kumagai et al., 2001; Yoneda and Hasezawa, 2003) have also been clarified in these cells. It is therefore envisaged that new findings on the regulation of secondary wall formation will be obtained through observations of microtubules in living cells.

The establishment of stable transformants of zinnia has not been reported, and there seem to be inherent difficulties in obtaining stable zinnia transformants. On the other hand, stable Arabidopsis transformants are easily obtainable. The use of Arabidopsis suspension cells will allow precise observations of microtubules in living cells. Furthermore, several genes involved in xylem development have already been identified in Arabidopsis mutants (Ye et al., 2002), and data from in vitro analyses of these genes will also soon be available. Therefore, the establishment of a tracheary element differentiation system using Arabidopsis cells will be an invaluable tool for the analysis of secondary wall development regulated by the cytoskeleton and also for furthering our understanding of the process of tracheary element differentiation.

For the reasons described above, we attempted to develop a tracheary element differentiation system using Arabidopsis cell suspensions. We first established a transgenic Arabidopsis cell suspension stably expressing a GFP-tubulin fusion protein and succeeded in differentiating them into tracheary elements. Based on the results, the roles of microtubules in secondary wall thickening are discussed.

RESULTS

Transformation of Arabidopsis Col-0 Cell Suspensions

To observe microtubules in living cells, we transformed Arabidopsis Col-0 cell suspensions with a vector containing a GFP(S65T)-tubulin fusion gene (Kumagai et al., 2001). This vector had been used successfully to observe microtubules time sequentially in living BY-2 cells and was thus judged suitable for our current purpose. As described in "Materials and Methods," the Col-0 cell suspensions were infected with the *Agrobacterium tumefaciens* harboring the vector. Consequently, 16 independent transformed cell lines, with clearly evident GFP fluorescence, were obtained. Among these, the fibers of microtubules were most distinctly observed in the cells of line number 13, and so these cells, designated AC-GT13 (Arabidopsis Col-0 cell suspension stably expressing a GFP-tubulin fusion protein no. 13), were used in observations of microtubules. In these AC-GT13 cells, there seemed to be no toxic effects of transformation since the cells showed the normal cell shapes and grew as well as the Col-0 cells (Fig. 1).

Establishment of the Differentiation System of Tracheary Elements from AC-GT13 Cells

To establish an efficient system of tracheary element differentiation from AC-GT13 cells, the cells were transferred into various media containing different concentrations of phytohormones, such as auxin, cytokinin, and brassinosteroid, which were thought to be related to tracheary element differentiation (Fukuda, 1997). As a result, we found that tracheary elements could be formed at higher frequencies when 7-d-old

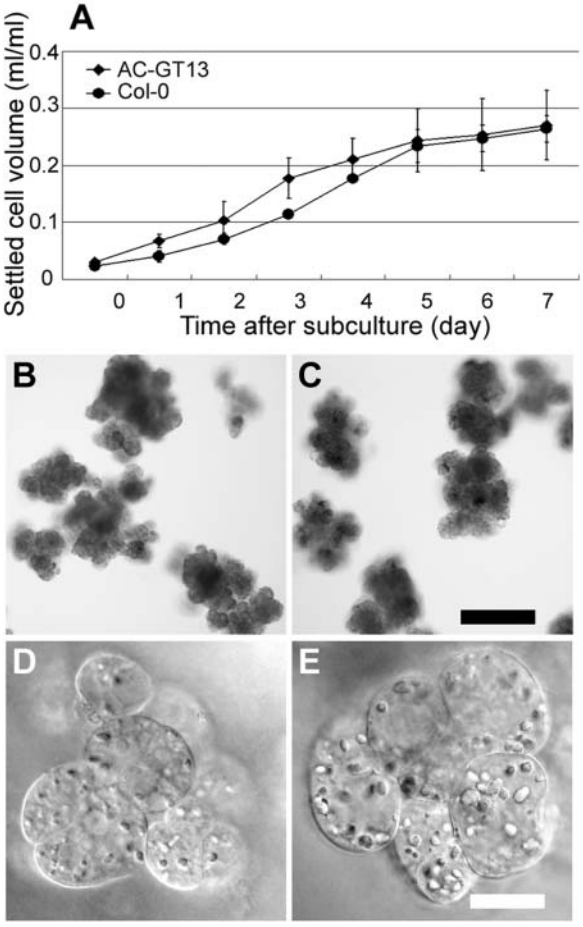

Figure 1. Characterization of AC-GT13 cells. A, Growth rate of AC-GT13 cells (diamonds) and Col-0 cell suspensions (circles). The settled cell volumes were measured in three independent experiments, and the means ± SD were plotted. B to E, The clumps and cells of Col-0 (B and D) and AC-GT13 (C and E) cells. Both cell lines consisted of clumps of 100 to 200 μm in diameter and involved cells with many granular structures. Bars = 200 μm (C) and 20 μm (E).

AC-GT13 cells were transferred into a modified Murashige and Skoog medium containing brassinolide (BL) but lacking 2,4-dichlorphenoxyacetic acid (2,4-D) and cultured in the dark (Fig. 2A). The obtained tracheary elements had distinct patterns of secondary wall deposition (Fig. 2B) that were similar to those of cultured zinnia mesophyll cells. The Col-0 cells also produced the tracheary elements undistinguishable from those of AC-GT13 cells (Fig. 2C). Hence, the tracheary elements formed in AC-GT13 cells were thought to be normal and typical tracheary elements. It was also found that the reduced concentrations of Suc (1%) and phosphate (170 mg L^{-1}) in the medium resulted in finer cell clumps that were suitable for observations.

The effects of 2,4-D and BL were investigated further. The tracheary element differentiation rates increased with increasing concentrations of BL up to 1 μM (Fig. 2D), while an opposite tendency was observed for 2,4-D (Fig. 2E). This clearly demonstrated an inhibitory effect of 2,4-D on tracheary element differentiation, and therefore the 2,4-D was removed by careful washing of the cells four times with 2,4-D-free medium and culturing them with 1 μM BL and various concentrations of 2,4-D. Consequently, a considerable improvement was seen in the differentiation rates, with no less than 30% of the cells becoming differentiated into tracheary elements after culturing without 2,4-D (Fig. 2F). To induce tracheary element differentiation, we therefore decided to culture the AC-GT13 cells with 1 μM BL after the removal of 2,4-D. In this differentiation system, cells with ambiguous secondary walls were scarcely observed and were not counted as tracheary elements.

Differentiation of Tracheary Elements from AC-GT13 Cells

To investigate when and how the tracheary elements were formed, cell sections were stained with toluidine blue and observed under a light microscope. Figure 3A shows the cells 48 h after the start of culture. Almost all the cells were rich in cytoplasm and were equally stained purple. However, the tracheary elements, recognized as blue-stained patterns of the secondary walls, appeared in the cells 72 h after culture (Fig. 3B). In cells 96 h after culture, an assembly of mature tracheary elements had been formed mainly in the inner cell clumps (Fig. 3C), although the tracheary elements had appeared occasionally on the surface of the cell clumps as shown in Figure 2.

The frequencies of tracheary elements at each period, as shown in Figure 3D, suggest that tracheary elements were formed semisynchronously from 48 to 96 h after culture. Finally, more than 30% of the cells had differentiated into tracheary elements after 120 h. We also tried to induce tracheary element differentiation using Col-0 cells, the parental cell line of AC-GT13, and the tracheary elements appeared in the similar time course as AC-GT13 cells, although the lower differentiation rates were obtained (data not shown). There is a possibility that the AC-GT13 cells had been cloned from a single cell that had the higher potential for tracheary element differentiation than other cells in the Col-0 cell suspension.

Observations of Microtubules during Secondary Wall Thickening

The AC-GT13 cells were able to stably express GFP-tubulin, through which microtubules could be observed in living cells. In AC-GT13 cells cultured in normal medium, the characteristic microtubule structures representing each stage of the plant cell cycle could be observed, and the same microtubule structures were also observed by immunofluorescent staining with anti-tubulin antibody (Supplemental Fig. 1). This indicated that the AC-GT13 cells were indeed suitable for microtubule observations. If the cells were observed 72 h after the beginning of culture in

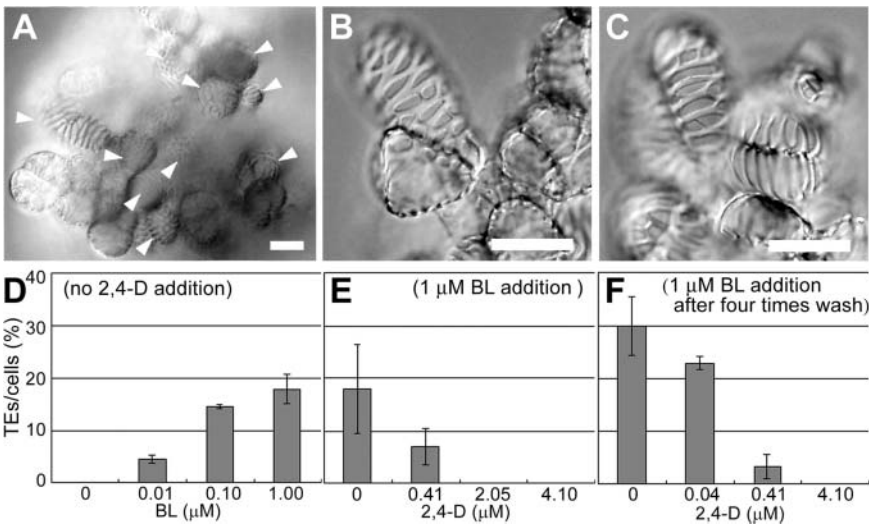

Figure 2. Tracheary element differentiation from AC-GT13 cells. A, AC-GT13 cells 168 h after induction of tracheary element differentiation. Tracheary elements (arrowheads) were found scattered throughout the cell clump. B and C, Tracheary elements with characteristic patterns of secondary wall deposition formed in AC-GT13 cells (B) and Col-0 cells (C). D, Effects of BL on the tracheary element differentiation rate after 168 h of culture. E, Effects of 2,4-D on the tracheary element differentiation rate after 168 h culture with 1 μM BL. F, Effects of removal of 2,4-D before the start of culture. Bars = 20 μm.

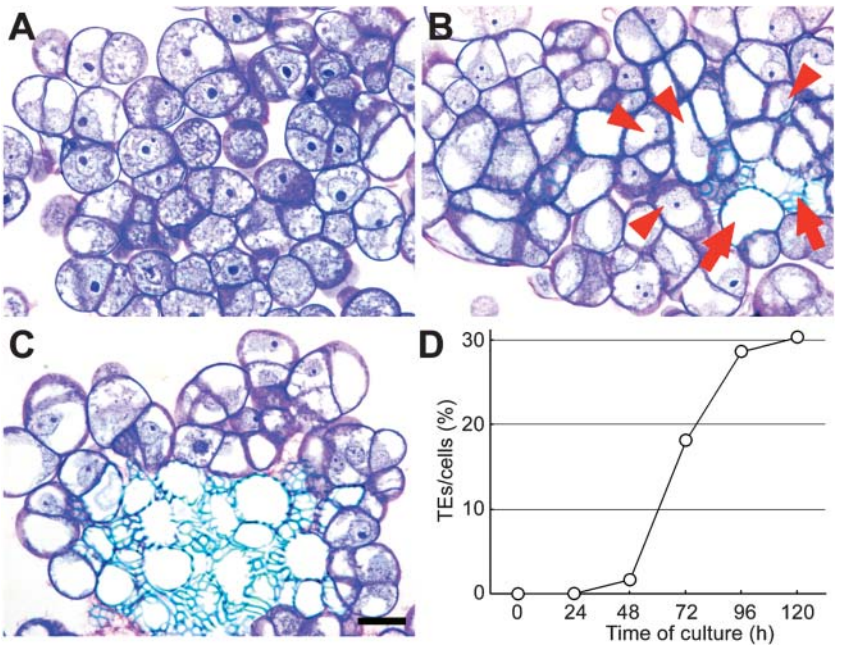

Figure 3. Development of tracheary elements in AC-GT13 cells. A, A toluidine blue-stained section of cells after 48 h of culture. The spots appearing dense blue are nucleoli. B, The secondary walls were observed in the cells after 72 h of culture. Arrows show mature tracheary elements lacking cytoplasm, and arrowheads show immature tracheary elements with cytoplasm and nuclei. Note that mature tracheary elements are surrounded by immature tracheary elements. C, Tracheary elements form an assembly in the cell clump after 96 h of culture. D, Time course of differentiation rates during the culture period. The frequency rapidly increased after 48 h of culture. Bar = 20 μm.

induction medium, another microtubule structure and secondary wall thickening began to be observed (Fig. 4). To obtain the highest resolution in microscopy, we selected and observed the cells in the most outer layers of the clumps. At first, the randomized cortical microtubules were observed (Fig. 4B, 0 h), and then the microtubules seemed to accumulate as broad bands (Fig. 4B, 2 h). Subsequently, the microtubule bundles appeared (Fig. 4B, 4 h, arrowhead) and the secondary wall thickening began to be seen at the same time and same position as the microtubule bundle (Fig. 4A, 4 h, arrow). Interestingly, at 6 h, the microtubule bundle seemed to be separately arranged into a pair of bundles that located along both sides of the secondary

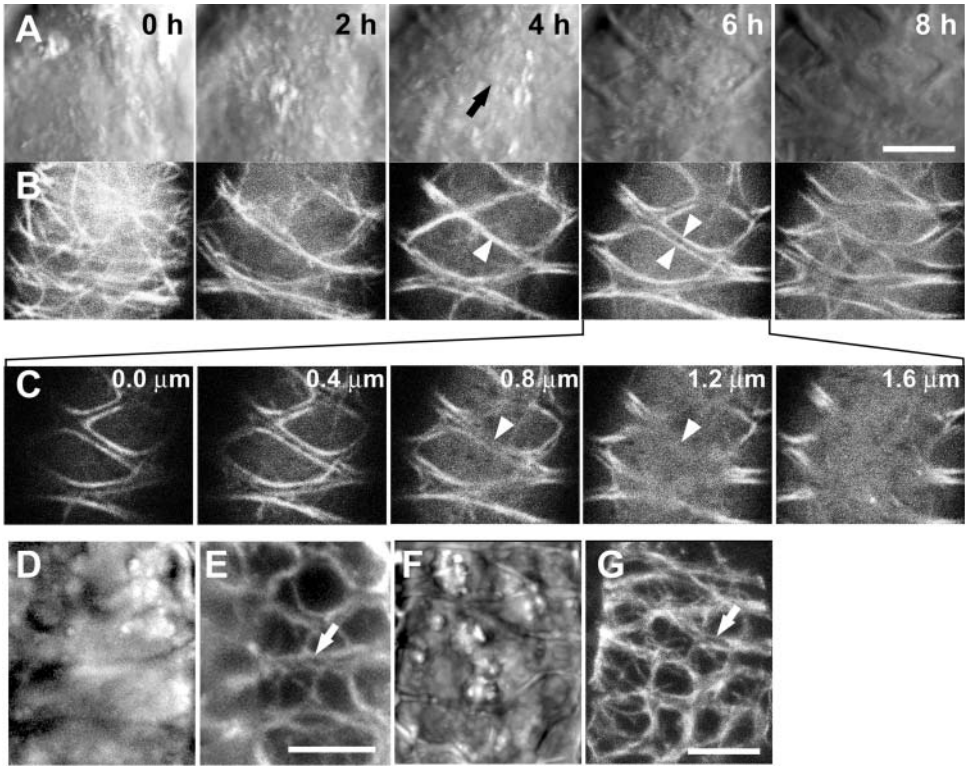

Figure 4. Time-sequential observations of AC-GT13 cells during secondary wall deposition. A and B, An AC-GT13 cell, transferred into a petri dish, was observed by CLSM at 2-h intervals in bright field (A) and GFP-tubulin (B). At each time point, five confocal optical sections were taken at 0.4-μm intervals and were reconstructed by maximum intensity projection. The black arrow shows appearance of secondary wall, and the arrowheads show microtubule bundles associated with secondary walls. C, The original confocal optical sections of B, 6 h. Microtubules were not observed under the secondary wall (arrowheads). D to G, Immunofluorescent microscopies of AC-GT13 cells with anti-tubulin antibody observed by a cooled CCD camera head system (D and E) and a CLSM system (F and G). Secondary wall deposition was recognized in bright fields (D and F), and the white arrows show the pairs of microtubule bundles in rhodamine signals (E and G). Bars = 5 μm.

wall (Fig. 4B, 6 h, arrowheads). This should be carefully interpreted because it is possible that the focus of the microscope couldn't reach the bottom of the secondary walls, and high background of cytosolic GFP signals might hide the microtubules just beneath the walls. However, the confocal sections shown in Figure 4C clearly reached the depth under the secondary walls, and microtubules were seldom observed beneath the secondary walls (Fig. 4C, arrowheads). The immunofluorescent microscopy, which had much lower background, also showed the microtubule bundles along both sides of the secondary walls (Fig. 4, D–G). These results demonstrate that the single microtubule bundle certainly split into two bundles, and each of them located along each side of the secondary wall.

Simultaneous Observations of Microtubules and Secondary Walls in Tracheary Element Development

The secondary walls could be stained with fluorescein-conjugated wheat germ agglutinin (WGA) that recognizes hemicelluloses (Hogetsu, 1990). To clarify the relationships between microtubules and secondary wall development, the secondary walls were stained with Texas Red-conjugated WGA so that the microtubules and secondary walls could be simultaneously observed (Fig. 5). WGA didn't inhibit tracheary element differentiation and secondary wall deposition in AC-GT13 cells (data not shown). At first, lateral secondary walls appeared and the microtubule bundles were orientated along both peripheries of the secondary walls. They also bridged longitudinally the lateral secondary walls (Fig. 5, arrowheads). Thereafter, nascent secondary walls emerged at sites where the bridges of the microtubule bundles had been localized and subsequently developed to bridge the lateral secondary walls. As the secondary wall bridges extended, the microtubule bundles separated into a pair of bundles on both sides of the secondary walls, as seen in Figure 4. The three-dimensional (3-D) structures of the secondary walls suggested that the secondary walls increased not only in their widths but also in their depths at the regions between the pairs of microtubule bundles where no microtubules could be recognized. As the secondary walls developed, the microtubule bundles became rearranged into circle-like structures and finally disappeared (Fig. 5, arrows).

Effects of Microtubule Inhibitors on Secondary Wall Formation

Tracheary elements formed from the AC-GT13 cells possessed various secondary wall patterns (Fig. 6, A–C). In previous studies, colchicine was used widely to investigate the function of microtubules during secondary wall deposition and was known to disorganize the secondary wall patterns (Pickett-Heaps, 1967; Hepler and Fosket, 1971; Fukuda and Komamine, 1980a). To make a comparison with them, 100 μM colchicine, a microtubule polymerization inhibitor, or

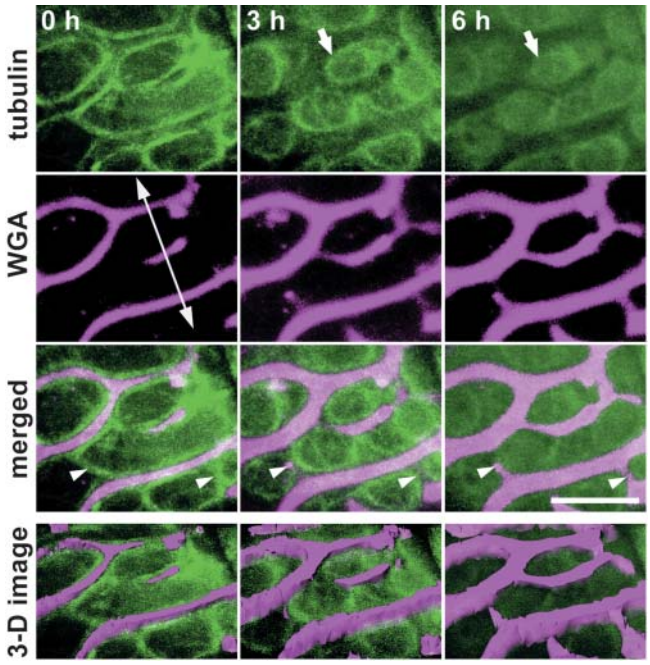

Figure 5. Time-sequential observations of microtubules and secondary walls. The secondary walls, stained by Texas Red-conjugated WGA, were simultaneously observed with the microtubules in a 72 h-cultured cell. Eight confocal optical sections were taken at 0.3-μm intervals and reconstructed by maximum intensity projection. The double-headed arrow represents the longitudinal axis of the cell. Arrowheads show the appearance of secondary wall bridges on the existing microtubule bundles. Arrows show the disappearing microtubule bundles. The 3-D images were reconstructed from the confocal images. Note that not only the width but also the thickness of the secondary walls was increased between the microtubule bundles. Bar = 5 μm.

2 μM taxol, a microtubule depolymerization inhibitor, was applied to the AC-GT13 cells at 48 h after the start of the culture period, when the secondary walls and microtubule bundles were rarely recognizable. On the colchicine addition, the secondary wall patterns turned rough, and the smooth rims of the secondary walls were destroyed (Fig. 6D). The abnormal secondary walls were also observed on the addition of propyzamide, another microtubule polymerization inhibitor (data not shown). By contrast, the taxol-treated tracheary elements tended to form simpler and oblique secondary wall patterns (Fig. 6, E and F). As higher inhibitor concentrations reduced the frequency of tracheary elements, these concentrations were adopted.

Then the inhibitors were added after the secondary walls and microtubule bundles had appeared. In the colchicine-treated cell, the smooth secondary walls became highly disordered by 8 h later, even though the pattern of the secondary wall itself was almost conserved (Fig. 7A). This suggests that the microtubule bundles that associated with both sides of the secondary walls were somehow stabilizing or equalizing secondary wall deposition. In the taxol-treated cell, the cytoplasmic GFP signals were extremely weak, reflecting the effects of taxol (Fig. 7B). To quantify the

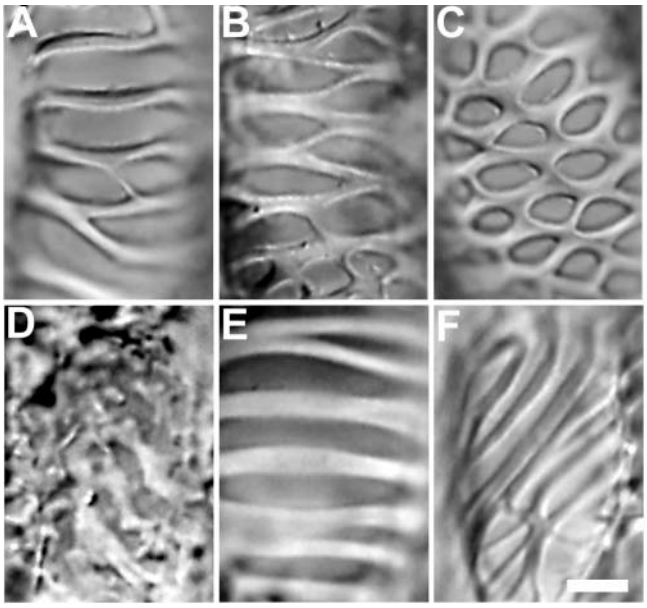

Figure 6. Patterns of secondary walls observed in AC-GT13 cells and the effects of microtubule inhibitors. A, A spiral pattern with a few bridges. The lateral secondary wall band extends around the cell to the neighbor band. B, A scalariform pattern. C, A reticulate pattern. D, Colchicine treatment after 48-h culture caused disorganized secondary wall patterns. E and F, Taxol treatment for 48-h culture caused simpler spiral and oblique secondary wall patterns. Bar = 5 μm.

effects of taxol on microtubule rearrangement, the distances between the pair of microtubule bundles were measured at 2-h intervals at three positions in each of three control and taxol-treated cells. In the taxol-treated cells, the distances were clearly shorter than those in the control cells (Fig. 7C), and their average velocity of microtubule bundle separation was two-thirds that of control cells (Fig. 7D). In the taxol-treated cells, the secondary walls were widening but the growth rate was clearly decreased and resulted in a narrower secondary wall band between the paired microtubule bundles (Fig. 7B). These results suggest that these microtubule bundles are essential not only in the determination of secondary wall patterns but also in the deposition of the secondary walls.

DISCUSSION

Tracheary Element Differentiation System Using Arabidopsis Cell Suspensions

Although several attempts were previously made to induce tracheary element differentiation, the only practical system available for the study of tracheary element differentiation has been that using zinnia mesophyll cells (Fukuda, 1992). In this study, we have succeeded in developing an in vitro system for tracheary element differentiation using a newly established transgenic Arabidopsis cell suspension, named AC-GT13, in which microtubules can be directly observed in investigations into microtubule orientations during tracheary element differentiation. The AC-GT13 cells differentiated into tracheary elements following culture in a medium free of 2,4-D but containing BL (Fig. 2). In this system, tracheary elements were semisynchronously formed during 48 to 96 h of culture, with more than 30% of the cells finally differentiating into tracheary elements (Fig. 3D). As far as we are aware, this is the only system available for tracheary element differentiation except for that using cultured zinnia mesophyll cells.

Interestingly, the tracheary elements tended to develop in a congregated manner (Fig. 3C) on the inside of cell clumps. There were several observations that tracheary elements were formed internally as nodules in other suspension cultures (Fukuda, 1992). Recently, Motose et al. (2004) revealed that intercellular communication is involved in tracheary element formation via an arabinogalactan protein named xylogen, which is emitted from the differentiating cells. Although such a tendency is a disadvantage for microscopic observations, we succeeded in reducing the size of the clumps by manipulating the concentration of Suc and phosphate.

The advantage of this system is its simple and reproducible culture preparation using repeatedly subcultured suspension cells without regenerating the culture from intact plants. Generally, callus or suspension cells tend to lose their potential for differentiation with time. It is surprising that there seems to be no significant reduction of the ability to reproduce tracheary elements more than 1 year after Col-0 cells were transformed into AC-GT13 cells. This indicates the availability of this system for the model system of tracheary element differentiation in the future.

Effects of Phytohormones on Tracheary Element Differentiation

Several phytohormones are known to participate in tracheary element differentiation (Kuriyama and Fukuda, 2001); notably, auxin is necessary for the differentiation process, and cytokinin promotes tracheary element differentiation. The AC-GT13 cells, however, required neither auxin nor cytokinin for tracheary element differentiation. In fact, the addition of 2,4-D reduced the frequencies of tracheary element differentiation (Fig. 2, E and F). This result appears to contradict previous concepts of a hormonal requirement for differentiation. However, Milioni et al. (2001) have reported that transient exposure to auxin and cytokinin is sufficient to induce differentiation in cultured zinnia mesophyll cells. In this context, it should be noted that the Arabidopsis Col-0, the original cell suspensions of the AC-GT13 cells, were derived from Arabidopsis (Columbia) roots by culturing with auxin and cytokinin, as described by Mathur et al. (1998).

Instead of auxin and cytokinin, AC-GT13 cells require brassinosteroid for tracheary element

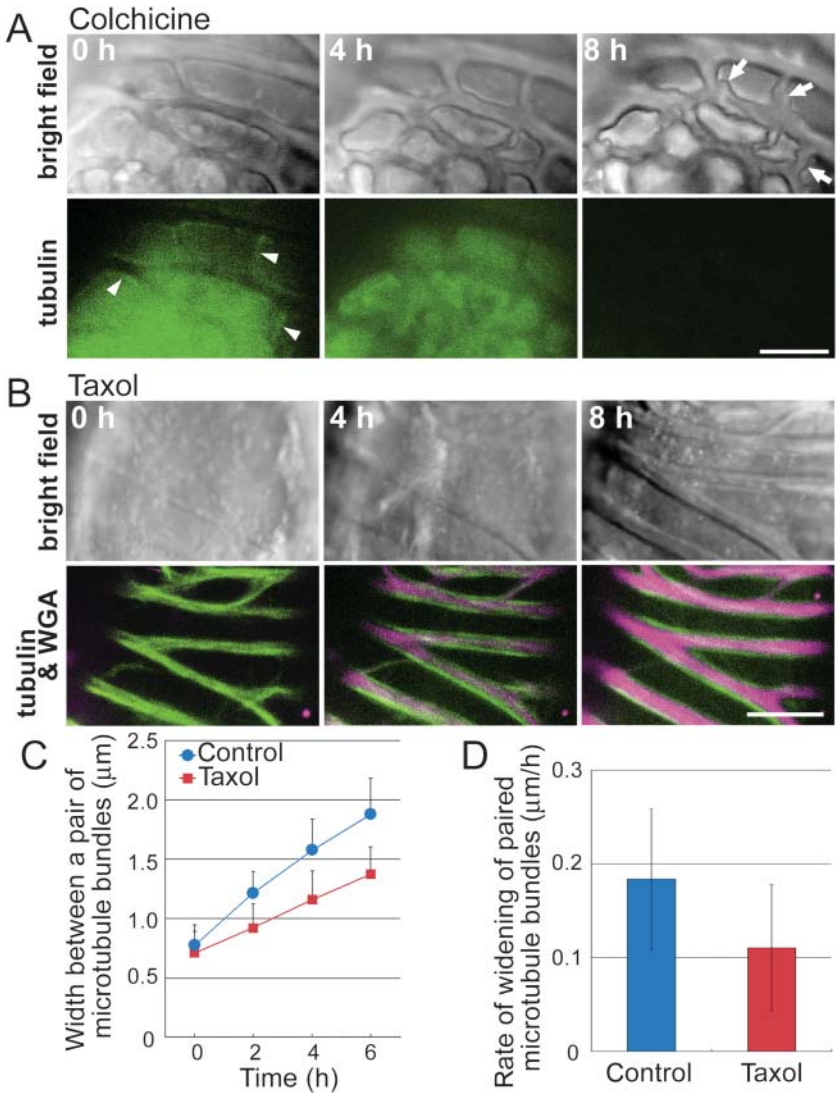

Figure 7. Effects of microtubule inhibitors on secondary wall thickening. A, AC-GT13 cells were treated with 100 μM colchicine, and observations were begun 30 min later. The microtubules could not be recognized except for a few short microtubule bundles shown by arrowheads. After 8 h of observation, the cells showed unequally deposited secondary walls (arrows). B, The AC-GT13 cells were inoculated with 2 μM taxol and with Texas Red-conjugated WGA to stain the secondary walls (magenta) and then time-sequentially observed after 60 min. Images shown are reconstructions of five optical confocal sections taken at 0.4-μm intervals. Note that secondary wall deposition was limited to between the pairs of microtubule bundles. C, The distances between each pair of microtubule bundles in a single cell were measured at three points, and the means ± SD of three cells were plotted. The distances between pairs of microtubule bundles in taxol-treated cells (squares) were narrower than those in control cells (circles). D, The rate of widening of the paired microtubule bundles was estimated from the results of C. Means ± SD for $n = 9$ are shown. The widening rate in taxol-treated cells was lower than that in control cells (Student's t test, $P < 0.05$). Bars = 5 μm.

differentiation. Brassinosteroids have been implicated in tracheary element differentiation. Cultured zinnia mesophyll cells synthesize high levels of brassinosteroids for themselves to enter into the final stages of differentiation (Yamamoto et al., 1997, 2001). In the AC-GT13 cells, exogenous BL, the final product of the brassinosteroid biosynthetic pathway, promoted a dose-dependent differentiation of tracheary elements (Fig. 2D). This suggests the importance of brassinosteroid as a general factor inducing tracheary element differentiation.

Other phytohormones, such as ethylene and abscisic acid, have also been associated with the tracheary element differentiation process (Kuriyama and Fukuda, 2001). The use of the AC-GT13 cell differentiation system may well contribute to our further understanding of the role of these hormones in tracheary element differentiation, which in turn may enable further improvements in the differentiation system.

Microtubule Behavior during Secondary Wall Development

Although the bundling of microtubules associated with secondary wall formation has been observed by transmission electron microscopy or indirect immunofluorescence microscopy in chemically fixed cells, data on the change of microtubule arrangement obtained by these studies are very limited. In this study, therefore, we adopted time-lapse imaging of microtubules in living AC-GT13 cells and showed that microtubules began to accumulate and microtubule bundles appeared before the secondary wall deposition (Fig. 4, A and B, 0 and 2 h). This is the apparent confirmation that microtubules appear at the site where secondary walls will deposit. Subsequently, a single bundle of microtubules under each secondary wall became separately arranged into two microtubule bundles that located along both sides of the nascent secondary wall. They moved apart concomitantly with

secondary wall development (Fig. 4, A and B, 4 and 6 h, arrowheads). Such microtubule bundles were also observed by the immunofluorescent microscopy (Fig. 4, E and G). Previously, the microtubules located beside the secondary walls were occasionally observed in cultured zinnia cells (Falconer and Seagull, 1988); however, the microtubules in living AC-GT13 cells are even smoother than those of fixed zinnia cells, resulting in clear exhibition of the paired microtubule bundles. Our observations have therefore directly elucidated the microtubule rearrangement with secondary wall development. It should be emphasized that such microtubule behavior was not previously clarified, despite continuous research for more than four decades. This clearly demonstrates the advantage of using the AC-GT13 cells for cytoskeletal investigations related to tracheary element differentiation.

The tracheary element differentiation system shown in this study has enabled us not only to observe the microtubules time sequentially but also to investigate the effect of microtubule inhibitors directly. The inhibition of widening of the paired microtubule bundles by taxol (Fig. 7, C and D) suggests that the microtubule bundles are rearranged not by sliding microtubules, but rather via polymerization and depolymerization of tubulin proteins, although the possibility still remains that the microtubule turnover is correlated with the rate of secondary wall deposition and thus taxol itself reduced secondary wall deposition.

Role of Microtubules in Secondary Wall Thickening

In differentiating zinnia mesophyll cells, irregularly patterned secondary walls would form if these microtubules were destroyed (Fukuda and Komamine, 1980b) or stabilized (Falconer and Seagull, 1985b). Similar results were also observed in the AC-GT13 cells (Fig. 6, D–F), whereas addition of microtubule inhibitors after the appearance of the microtubule bundles resulted in no changes in the secondary wall patterns. However, the smooth morphology of the secondary walls became rough in colchicine-treated cells, and narrow secondary walls developed in between the microtubule bundles in taxol-treated cells. These observations suggest that the microtubule bundles play an important role in secondary wall thickening.

How do these microtubule bundles regulate secondary wall thickening? In the bordered pits of tracheids, the microtubules were found to accumulate along the edge of the pits in the secondary walls (Hogetsu, 1991; Uehara and Hogetsu, 1993; Chaffey et al., 1997, 1999; Funada et al., 2001). Hogetsu (1991) hypothesized that these microtubules determined the boundary of the secondary walls by separating the plasma membrane into two domains: the domain under the secondary wall having a specialized affinity for some vesicles and able to activate the cellulose synthase complexes. Recently, in Arabidopsis, cellulose synthases specific to the secondary walls were isolated (Taylor et al., 1999, 2000, 2003) and shown to be localized under the secondary walls only when they could form the complete complexes (Gardiner et al., 2003). It is possible that these secondary wall-specific cellulose synthases cooperate with the specialized plasma membranes beneath the secondary walls.

Another possibility is that the secondary walls in AC-GT13 cells may be relatively flat and broad, and the microtubules preferentially accumulate at the sides of the secondary wall ingrowths to regulate active cellulose synthase complexes and/or to deliver vesicles. Previous studies of microtubules and secondary walls in vivo were largely in cylindrical xylem cells. In comparison to them, AC-GT13 cells are somehow spherical, and thus it is expected that such secondary wall development and paired microtubule bundles as observed in this study may be seen in noncylindrical parenchyma cells that are redifferentiating into tracheary elements in vivo. In any case, the 3-D images shown in Figure 5 didn't have enough resolution to demonstrate them. More accurate 3-D reconstruction of secondary wall structures and precise analysis of secondary wall development will resolve this problem.

Sequential Development of Secondary Wall

The sequential development of secondary walls from simple patterns to complex scalariform or reticulate patterns was suggested previously from observations of cultured zinnia mesophyll cells (Falconer and Seagull, 1988). Time-sequence observations of the microtubules and secondary walls in the AC-GT13 cells directly demonstrated that preceding microtubule bundles guided the longitudinal secondary wall bridge formation later than the lateral secondary walls. Moreover, we showed that secondary wall bridge formation itself seems to be regulated by the microtubules, as with lateral secondary walls, since similar microtubule behavior was observed (Fig. 5).

CONCLUSION

In this study, we have established a system for tracheary element differentiation using the transgenic Arabidopsis cell suspension AC-GT13. Approximately 30% of the cells could semisynchronously differentiate into tracheary elements after 96 h of culture in induction medium. As far as we are aware, this currently is the only system, except for the one in zinnia, available for biochemical or molecular analyses of tracheary element differentiation. We are therefore confident that this system will contribute to the further analysis of processes involved in tracheary element differentiation, especially in secondary wall development.

The sequential observation of microtubules in the AC-GT13 cells revealed novel microtubule behavior associated with secondary wall development. The fact

that such behavior was not previously recognized, despite the numerous studies conducted on microtubules and secondary walls, clearly demonstrates the superiority of the AC-GT13. Further observations will clarify the processes of microtubule bundling and separation involved in tracheary element differentiation.

MATERIALS AND METHODS

Plant Cell Culture

Arabidopsis (*Arabidopsis thaliana*) Col-0 cells were kindly provided by Dr. Masaaki Umeda. The origin of the Col-0 cells has been described by Mathur et al. (1998). Col-0 cells were cultured in 20 mL of modified Murashige and Skoog medium, pH 5.8, containing 4.33 g L^{-1} of Murashige and Skoog inorganic salts, 4.1 μM 2,4-D, 3.0% (w/v) Suc, 510 mg L^{-1} KH_2PO_4, and 2× B5 vitamins including 2 mg L^{-1} nicotinic acid, 2 mg L^{-1} pyridoxine-HCl, 20 mg L^{-1} thiamine-HCl, and 200 mg L^{-1} myoinositol. The cells were agitated on a rotary shaker at 130 rpm at 23°C in a 16-h-light/8-h-dark period. At weekly intervals, 2-mL aliquots of the culture were transferred to 20 mL of fresh medium in 100-mL culture bottle jars.

Stable Transformation of Arabidopsis Col-0 Cell Suspensions

A 1-mL aliquot of 3-d-old cell suspensions of Arabidopsis Col-0 was added to 3 mL of fresh medium and then inoculated with 100 μL of an overnight culture of *Agrobacterium tumefaciens* strain LBA4404, transformed with a GFP(S65T)-tubulin alpha (TUA) vector construct (Kumagai et al., 2001) as described by An (1985). After a 2-d incubation at 23°C, the Arabidopsis cells were washed four times with 5 mL of fresh medium and then plated onto a solid, modified Murashige and Skoog medium containing 0.4% (w/v) gellam gum, 500 mg L^{-1} clafolan, and 100 mg L^{-1} kanamycin sulfate. The calluses that appeared after 3 weeks were transferred onto new plates and subsequently cultured independently. Each callus of about 1 cm in diameter was transferred into 20 mL of liquid modified Murashige and Skoog medium in 100-mL culture bottles and agitated on a rotary shaker at 130 rpm at 23°C in the dark. After 2 weeks, cell lines were selected by identifying GFP-fluorescent cells by fluorescence microscopy. The cell line most suitable for microtubule observations was designated Arabidopsis Col-0 cell suspension stably expressing a GFP-tubulin fusion protein number 13 (AC-GT13) and was maintained by the same method described above.

Induction of Tracheary Element Differentiation from AC-GT13 Cells

A 1-mL aliquot of 7-d-old AC-GT13 cells was washed four times with induction medium, pH 5.8, containing 4.33 mg L^{-1} Murashige and Skoog inorganic salts, 170 mg L^{-1} KH_2PO_4, 1.0% (w/v) Suc, and 2× B5 vitamins. The cells were then transferred into 10 mL of fresh induction medium, including 1 μM BL in 100-mL culture bottle jars, and then agitated on a rotary shaker at 130 rpm at 23°C in the dark.

Anatomy of Tracheary Elements and Measurement of Differentiation Rates

The suspension cells were fixed every 24 h after the beginning of induction in a mixture of 45% ethanol, 2.5% acetic acid, and 2.5% (v/v) formalin and rinsed twice with 0.1 M phosphate-buffered saline (PBS; pH 7.0). The cells were dehydrated in a graded series of ethanol (50, 60, 70, 80, 90, 99.5, and 100% [v/v] for 20 min for each step) and embedded in technovit 7100 resin (Kulzer & Co., Wehrheim, Germany). The 0.4-μm-thick sections, cut with an ultramicrotome (Ultracut UCT; Leica Microsystems, Wetzlar, Germany), were stained for 1 min with 0.1% (w/v) Toluidine Blue O (Waldeck GmbH & Co., Munster, Germany) solution in 100 mM PBS, pH 7.0, rinsed with distilled water, and then observed under a light microscope (BX51; Olympus, Tokyo). For measurement of differentiation rates, three sections were independently cut from one sample, and more than 500 cells were examined in each section.

Immunocytochemistry and Cell Staining

For immunostaining, cells were fixed with 3.7% (v/v) formaldehyde in 50 mM PIPES, 1 mM $MgSO_4$, 5 mM EGTA, and 1% (v/v) glycerol, pH 6.8, for 30 min at room temperature and then treated with an enzyme solution containing 0.5% (w/v) pectolyase and Y23 cellulase Y-C (both from Seishin, Tokyo) in 0.4 M mannitol, 50 mM PIPES, 1 mM $MgSO_4$, 5 mM EGTA, 0.5 mM phenylmethylsulfonyl fluoride, and 1 mg L^{-1} leupeptin. Then cells were attached to polyethylenimine-coated coverslips. The cells were incubated in 0.1 M Gly, 1% (w/v) bovine serum albumin, and 0.05% (v/v) Triton X-100 in PBS (20 mM sodium phosphate and 150 mM NaCl, pH 7.0) for 15 min and incubated for 1 h with the primary antibody mouse anti-chicken α-tubulin (Oncogene, Darmstadt, Germany) in PBS. The specimens were then washed three times in PBS and incubated for 1 h with the secondary antibody rhodamine-conjugated goat anti-mouse antibody (Cappel, West Chester, PA). Then cells were washed three times with PBS and embedded in a glycerol solution containing an antifading reagent (SlowFade Light; Molecular Probes, Eugene, OR).

Microscopy

For the time-sequence observations, 72-h-old AC-GT13 cells, cultured in induction medium with 1 μM BL, were transferred onto 35-mm petri dishes with 27-mm coverslip windows at the bottom (Matsunami Glass Industries, Osaka). The dishes were placed onto the inverted platform of a fluorescence microscope (IX; Olympus), equipped with an UPlanApo 100×/1.35 oil Iris objective lens and a confocal laser scanning head and control systems (CLSM GB-200; Olympus). This observation system was found to be useful for the observation of microtubules in AC-GT13 cells with developing secondary walls. Moreover, by inoculation of the cells with 20 mg L^{-1} Texas Red-conjugated WGA (Molecular Probes; 2 mg mL^{-1} stock solution in distilled water) for 30 min before the observations, the microtubules and secondary walls could be followed simultaneously.

GFP was excited by argon laser (wavelength 488 nm), Texas Red and rhodamine were excited by helium neon laser (wavelength 543 nm), and each scan of single-confocal sections took 10 s by a confocal laser scanning microscopy (CLSM) system. The confocal sections were reconstructed by maximum-intensity projection using Metamorph (Universal Imaging, Downingtown, Panama) and processed digitally using Photoshop software (Adobe Systems, Mountain View, CA). For the analysis of the 3-D structures of the secondary walls, images were reconstructed using Amira (Indeed-Visual Concepts GmbH, Berlin).

For the observations of immunostained cells, a fluorescence microscope (IX; Olympus) equipped with a cooled CCD camera head system (Cool-SNAP HQ, PhotoMetrics, Huntington Beach, Canada) were also used in addition to the CLSM system described above.

Inhibitor Treatments

After 72 h of culture in induction medium, the AC-GT13 cells were treated with 2 μM taxol (Sigma, St. Louis) or 100 μM colchicine (Sigma), following staining of the secondary walls with WGA, and were then observed 30 or 60 min later by CLSM.

ACKNOWLEDGMENTS

We thank Dr. Csaba Koncz (Max-Planck-Institut für Züchtungsforschung) and Dr. Masaaki Umeda (The University of Tokyo) for providing the Arabidopsis Col-0 cell suspension, and Dr. Hiroo Fukuda (The University of Tokyo) for valuable suggestions. We also thank Arata Yoneda (The University of Tokyo) for technical advice.

Received September 7, 2004; returned for revision November 1, 2004; accepted December 28, 2004.

LITERATURE CITED

An G (1985) High efficiency transformation of cultured tobacco cells. Plant Physiol **79:** 568–570

Brower DJ, Hepler PK (1976) Microtubules and secondary wall deposition in xylem: the effects of isopropyl N-phenylcarbamate. Protoplasma **87:** 91–111

Chaffey NJ, Barnett JR, Barlow PW (1997) Cortical microtubule involvement in bordered pit formation in secondary xylem vessel elements of *Aesculus hippocastanum* L. (Hippocastanaceae): a correlative study using electron microscopy and indirect immunofluorescence microscopy. Protoplasma **197:** 64–75

Chaffey NJ, Barnett JR, Barlow PW (1999) A cytoskeletal basis for wood formation in angiosperm trees: the involvement of cortical microtubules. Planta **208:** 19–30

Falconer MM, Seagull RW (1985a) Immunofluorescent and calcofluor white staining of developing tracheary elements in *Zinnia elegans* L. suspension cultures. Protoplasma **125:** 190–198

Falconer MM, Seagull RW (1985b) Xylogenesis in tissue culture: taxol effects on microtubule reorientation and lateral association in differentiating cells. Protoplasma **128:** 157–166

Falconer MM, Seagull RW (1988) Xylogenesis in tissue culture III: continuing wall deposition during tracheary element differentiation. Protoplasma **144:** 10–16

Fukuda H (1992) Tracheary element formation as a model system of cell differentiation. Int Rev Cytol **136:** 289–332

Fukuda H (1997) Tracheary element differentiation. Plant Cell **9:** 1147–1156

Fukuda H, Kobayashi H (1989) Dynamic organization of the cytoskeleton during tracheary-element differentiation. Dev Growth Differ **31:** 9–16

Fukuda H, Komamine A (1980a) Establishment of an experimental system for the study of tracheary element differentiation from single cells isolated from the mesophyll of *Zinnia elegans.* Plant Physiol **65:** 57–60

Fukuda H, Komamine A (1980b) Direct evidence for cytodifferentiation to tracheary elements without intervening mitosis in a culture of single cells isolated from the mesophyll of *Zinnia elegans.* Plant Physiol **65:** 61–64

Funada R, Mimura H, Shibagaki M, Furusawa O, Miura T, Fukatsu E, Kitin P (2001) Involvement of localized cortical microtubules in the formation of a modified structure of wood. J Plant Res **114:** 491–497

Gardiner JC, Taylor NG, Turner SR (2003) Control of cellulose synthase complex localization in developing xylem. Plant Cell **15:** 1740–1748

Hardham AR, Gunning BES (1979) Interpolation of microtubules into cortical arrays during cell elongation and differentiation in roots of *Azolla pinnata.* J Cell Sci **37:** 411–442

Hardham AR, Gunning BES (1980) Some effects of colchicine on microtubules and cell division in roots of *Azolla pinnata.* Protoplasma **102:** 31–51

Hasezawa S, Ueda K, Kumagai F (2000) Time-sequence observations of microtubule dynamics throughout mitosis in living cell suspensions of stable transgenic *Arabidopsis*: direct evidence for the origin of cortical microtubules at M/G_1 interface. Plant Cell Physiol **41:** 244–250

Hepler PK (1981) Morphogenesis of tracheary elements and guard cells. Cell Biol Monogr **8:** 327–347

Hepler PK, Fosket DE (1971) The role of microtubules in vessel member differentiation in *Coleus.* Protoplasma **72:** 213–236

Hepler PK, Newcomb EH (1964) Microtubules and fibrils in the cytoplasm of *Coleus* cells undergoing secondary wall deposition. J Cell Biol **20:** 529–533

Hogetsu T (1990) Detection of hemicelluloses specific to the cell wall of tracheary elements and phloem cells by fluorescein-conjugated lectins. Protoplasma **156:** 67–73

Hogetsu T (1991) Mechanism for formation of the secondary wall thickening in tracheary elements: microtubules and microfibrils of tracheary elements of *Pisum sativum* L. *and Commelina communis* L. and the effects of amiprophosmethyl. Planta **185:** 190–200

Kumagai F, Yoneda A, Tomida T, Sano T, Nagata T, Hasezawa S (2001) Fate of nascent microtubules organized at the M/G_1 interface, as visualized by synchronized tobacco BY-2 cells stably expressing GFP-tubulin: time-sequence observations of the reorganization of cortical microtubules in living plant cells. Plant Cell Physiol **42:** 723–732

Kuriyama H, Fukuda H (2001) Regulation of tracheary element differentiation. J Plant Growth Regul **20:** 35–51

Mathur J, Szabados L, Schaefer S, Grunenberg B, Lossow A, Jonas-Straube E, Schell J, Koncz C, Koncz-Kalman Z (1998) Gene identification with sequenced T-DNA tags generated by transformation of *Arabidopsis* cell suspension. Plant J **13:** 707–716

Milioni D, Sado PE, Stacey NJ, Domingo C, Roberts K, McCann MC (2001) Differential expression of cell-wall-related genes during the formation of tracheary elements in the Zinnia mesophyll cell system. Plant Mol Biol **47:** 221–238

Motose H, Sugiyama M, Fukuda H (2004) A proteoglycan mediates inductive interaction during plant vascular development. Nature **429:** 873–878

Pickett-Heaps JD (1966) Incorporation of radioactivity into wheat xylem walls. Planta **71:** 1–14

Pickett-Heaps JD (1967) The effects of colchicine on the ultrastructure of dividing plant cell, xylem wall differentiation and distribution of cytoplasmic microtubules. Dev Biol **15:** 206–236

Pickett-Heaps JD, Northcote DH (1966) Relationship of cellular organelles to the formation and development of the plant cell wall. J Exp Bot **17:** 20–26

Shaw SL, Kamyar R, Ehrhardt DW (2003) Sustained microtubule treadmilling in *Arabidopsis* cortical arrays. Science **300:** 1715–1718

Taylor NG, Howells RM, Huttly AK, Vickers K, Turner SR (2003) Interactions among three distinct CesA proteins essential for cellulose synthesis. Proc Natl Acad Sci USA **100:** 1450–1455

Taylor NG, Laurie S, Turner SR (2000) Multiple cellulose synthase catalytic subunits are required for cellulose synthesis in *Arabidopsis.* Plant Cell **12:** 2529–2539

Taylor NG, Scheible WR, Cutler S, Somerville CR, Turner SR (1999) The *irregular xylem3* locus of *Arabidopsis* encodes a cellulose synthase required for secondary cell wall synthesis. Plant Cell **11:** 769–779

Ueda K, Matsuyama T (2000) Rearrangement of cortical microtubules from transverse to oblique or longitudinal in living cells of transgenic *Arabidopsis thaliana.* Protoplasma **213:** 28–38

Ueda K, Sakaguchi S, Kumagai F, Hasezawa S, Quader H, Kristen U (2003) Development and disintegration of phragmoplasts in living cultured cells of a GFP::TUA6 transgenic *Arabidopsis thaliana* plant. Protoplasma **220:** 111–118

Uehara K, Hogetsu T (1993) Arrangement of cortical microtubules during formation of bordered pit in the tracheids of *Taxus.* Protoplasma **172:** 145–153

Wooding FBP, Northcote DH (1964) The development of the secondary wall of the xylem in *Acer pseudoplantanus.* J Cell Biol **23:** 327–337

Yamamoto R, Demura T, Fukuda H (1997) Brassinosteroids induce entry into the final stage of tracheary element differentiation in cultured *Zinnia* cells. Plant Cell Physiol **38:** 980–983

Yamamoto R, Fujioka S, Demura T, Takatsuto S, Yoshida S, Fukuda H (2001) Brassinosteroid levels increase drastically prior to morphogenesis of tracheary elements. Plant Physiol **125:** 556–563

Ye ZH (2002) Vascular tissue differentiation and pattern formation in plants. Annu Rev Plant Biol **53:** 183–202

Ye ZH, Freshour G, Hahn MG, Burk DH, Zhong RQ (2002) Vascular development in *Arabidopsis.* Int Rev Cytol **220:** 225–256

Yoneda A, Hasezawa S (2003) Origin of cortical microtubules organized at M/G_1 interface: recruitment of tubulin from phragmoplast to nascent microtubules. Eur J Cell Biol **82:** 461–471

Yoneda A, Kutsuna N, Hasezawa S (2003) Dynamic organization of microtubules and vacuoles visualized by GFP in living plant cells. Recent Res Dev Plant Mol Biol **1:** 127–137